ORIGINAL ARTICLE

An operational methodology for determining relevant DRASTIC factors and their relative weights in the assessment of aquifer vulnerability to contamination

Lamine Boumaiza[1,2] · Julien Walter[1,2] · Romain Chesnaux[1,2] · Karthikeyan Brindha[3] · Lakshmanan Elango[4] · Alain Rouleau[1,2] · Przemyslaw Wachniew[5] · Christine Stumpp[6]

Abstract

The DRASTIC index used to assess the vulnerability of aquifers to contamination, has been subject to various adjustments to improve its reliability. These adjustments include adding and/or eliminating certain aquifer factors and modifying the factor weights. Nonetheless, there is no consensus about which factors, or their respective weights, are most important for assessing aquifer vulnerability. In the present study, we propose an operational methodology that: (1) identifies the relevant factors for assessing aquifer vulnerability to contamination; and (2) determines the relative importance of the selected factors. We applied this approach to a large data set of granular aquifers from a region in Canada, which includes information for DRASTIC factors, combined with groundwater quality and land-use data. We found that for our study region, topography (terrain-slope) is an irrelevant factor for assessing the vulnerability of aquifers to contamination. On the other hand, the relevant factors ranked according to their relative importance (from highest to lowest), are (1) water table depth; (2) hydraulic conductivity; (3) characteristics of vadose zone materials; and (4) recharge. Our approach can serve as an initial step for identifying the relevant aquifer factors when assessing aquifer vulnerability and determining the relative importance of the relevant factors to validate weights attributed to these factors. Our methodology can help adapt index-based methods of aquifer vulnerability assessment to a range of study regions.

Keywords Hydrogeology · Groundwater · DRASTIC · Water quality index · Land-use · Canada

Introduction

Groundwater of sufficient quantity and quality is often available within the subsurface of large geological systems. However, the uncontrolled or unsustainable exploitation of groundwater in combination with anthropogenic activities on the land surface—especially if linked with inadequate changes in land use—can lead to a rapid and severe deterioration of groundwater quality (Bouchaou et al. 2008; Valle Junior et al. 2014; Erostate et al. 2018; Zendehbad et al. 2019; Boumaiza et al. 2020a). To determine the sensitivity of groundwater to potential anthropogenic contamination, resource managers often rely on aquifer vulnerability assessment. This evaluation is essential for implementing effective groundwater management strategies and for raising public awareness about the risk of groundwater contamination. Aquifer vulnerability is related to potential contamination pathways or any other pressures between the groundwater source and potential receptors (Foster et al. 2013).

✉ Lamine Boumaiza
lamine.boumaiza@uqac.ca

1 Département des Sciences Appliquées, Université du Québec à Chicoutimi, Saguenay, Québec G7H 2B1, Canada

2 Centre d'études sur les Ressources Minérales, Groupe de Recherche Risque Ressource Eau, Université du Québec à Chicoutimi, Saguenay, Québec G7H 2B1, Canada

3 Hydrogeology Group, Institute of Geological Sciences, Freie Universität Berlin, 12249 Berlin, Germany

4 Department of Geology, Anna University, Chennai 600 025, India

5 Faculty of Physics and Applied Computer Science, AGH University of Science and Technology, 30-059 Krakow, Poland

6 Institute for Soil Physics and Rural Water Management, University of Natural Resources and Life Sciences, 1190 Vienna, Austria

This vulnerability may be divided into two categories: (1) intrinsic, which considers the physical properties of the aquifer system, i.e., intrinsic geological and hydrogeological characteristics, independent of the nature of the contaminants (Gogu and Dassargues 2000); and (2) specific, which is dependent on contaminant properties, i.e., physical and biogeochemical attenuation processes, and the physical properties of the aquifer system (Doerfliger et al. 1999). Various methods for assessing aquifer vulnerability have been developed, and these methods have been reviewed in multiple papers (Gogu and Dassargues 2000; Shirazi et al. 2012; Kumar et al. 2015; Wachniew et al. 2016; Iván and Mádl-Szőnyi 2017; Machiwal et al. 2018). Machiwal et al. (2018), in a comprehensive review, identified three types of aquifer vulnerability assessment: (1) index-based methods, (2) statistical-based methods, and (3) process-based methods. Index-based methods can be further separated into two groups, depending on their applicability to either granular or karst aquifers. The commonly used granular porous aquifer index-based methods include DRASTIC (Aller et al. 1987), GOD (Foster 1987), AVI (Van Stempvoort et al. 1993), SINTACS (Civita and De Maio 2004), ISIS (Gogu and Dassargues 2000), and SEEPAGE (Moore and John 1990). Index-based methods incorporate various factors that are related to the characteristics of contaminant transport through the unsaturated and saturated zones.

The ratings and relative weights of factors, used to assess the aquifer vulnerability, are subjective and have been modified for different case studies; such modifications also included adding and/or ignoring some factors. DRASTIC is one of the most widely used index-based approaches for assessing aquifer vulnerability (e.g., Fritch et al. 2000; Ibe et al. 2001; Baalousha 2006; Saibi and Ehara 2008; Awawdeh and Jaradat 2010; Brindha and Elango 2015; Sadiki et al. 2018). The DRASTIC factors are depth to water table (D), recharge (R), aquifer media (A), soil media (S), topography (T), the impact of the vadose zone (I), and hydraulic conductivity (C) (Aller et al. 1987). The use or interpretation of these factors varies markedly among case studies. For example, Zhou et al. (2010) proposed an adapted DRAV index in which they removed the topography factor (T) and replaced soil type (S) and hydraulic conductivity (C) by a vadose zone lithology factor (V). This DRAV index was considered more adapted to arid regions characterized by limited runoff. Liggett and Allen (2011) modified the DRASTIC factor ratings to account for a site-specific lithology; the soil drainage was incorporated into the soil media factor (S) and topography (T). These modifications provided a more detailed map of aquifer vulnerability to contamination for a given study aquifer than when using the original DRASTIC index. The DRASTIC factors have also been adjusted for specific settings. For example, Wang et al. (2007) developed DRAMIC (a DRASTIC-derived index) for use in urban settings. In DRAMIC, the soil type factor (S) and topography (T) are substituted by the factor (M), which considers aquifer thickness. They also replaced the hydraulic conductivity factor by contaminant impact, denoted by the letter (C). Justification for the use of this adapted index includes (1) cities often being built on relatively flat areas, thereby reducing the importance of topography and (2) the concrete ground-surface covering in urban areas that often limits the available information about the characteristics of the underlying soil. Singh et al. (2015) introduced an anthropic factor (A) to the original DRASTIC index to incorporate the anthropogenic influence in urbanized environments. Their adapted index, DRASTICA, gave much weight to the added anthropic factor (A) because they assumed its effect on vulnerability was similar to that for the factors of water-depth and vadose zone material. The factors and weightings used in a DRASTIC-based vulnerability assessment can also be varied to take into account the effects of land use on groundwater contamination. For example, Panagopoulos et al. (2006) used the correlation coefficient of each DRASTIC factor with the nitrate concentration in groundwater to evaluate the ratings and weights of all DRASTIC factors. They observed, similar to other studies (Rosen 1994; McLay et al. 2001), that the factors of hydraulic conductivity (C) and soil type (S) had no influence on nitrate concentrations in groundwater. Hence, the hydraulic conductivity and soil type factors were removed from the DRASTIC index, whereas they incorporated land use. Ruopu et al. (2014) also deemed land use to be relevant when assessing aquifer vulnerability and proposed the DRASTIL index (where L refers to land use). Other researchers have also added land use as a factor to the original DRASTIC index (Al-Hanbali and Kondoh 2008; Heiß et al. 2020). Chenini et al. (2015) studied the vulnerability of aquifers to contamination by assuming that only factors related to the vadose zone are involved in vertical contaminant transport. They, therefore, adapted the DRIST index, derived from DRASTIC, by eliminating aquifer type (A) and hydraulic conductivity (C). Guo et al. (2007) numerically evaluated the rating values and weights of DRASTIC and other related factors. They identified soil type (S), topography (T), and the impact of the vadose zone (I) as factors that could be ignored, whereas they found that other factors, including the ratio of cumulative thickness of clay layers to the total thickness of vadose zone and the contaminant adsorption coefficient of sediment in the vadose zone, to be relevant when assessing aquifer vulnerability to contamination. Other DRASTIC-derived index alternatives have proposed vulnerability indices more adapted to specific properties, e.g., a modified DRASTIC for pesticide contamination and a modified DRASTIC specific to nitrate in aquifers, for which factor weights were modified from those in the original DRASTIC index (Huan et al. 2012; Neshat et al. 2014; Saha and Alam 2014; Fusco et al. 2020).

Several studies have relied on the establishment of a linear correlation between nitrate concentration and vulnerability maps to validate the approach used to assess aquifer vulnerability (e.g., Panagopoulos et al. 2006; Kazakis and Voudouris 2015; Arauzo 2017; Shrestha et al. 2017). Pacheco et al. (2018) demonstrated the poor applicability of such a correlation as a validation process, because the dynamics of nitrate within aquifers can be dominated by lateral flow; a dynamic assumed to be negligible in vulnerability assessment methods.

Modifications of factors and weights for the DRASTIC-derived indices can be justified given that the assessed vulnerability based on the original DRASTIC index is often considered to be unsatisfactory (Al-Zabet 2002; Pacheco and Sanches Fernandes 2013; Pacheco et al. 2015). A variety of statistical techniques, ranging from a simple linear regression to complex statistical techniques, have been utilized to describe the importance of a factor relative to the others. Some studies (e.g., Javadi et al. 2011) are based on correlation analysis between factor and nitrate concentrations in groundwater. Others have used the single parameter sensitivity analysis based on subarea conditions that can be identified by GSI (e.g., Hasiniaina et al. 2010). The Analytic Hierarchy Process assessment method has been also used in many studies (e.g., Sener and Davraz 2013). This technique normalizes the assigned weights to factors using the eigenvector technique, which reduces the subjectivity involved in the initial assigned weights. The practice of applying fuzzy logic statistical methods is also increasingly used in vulnerability assessments using the DRASTIC index (e.g., Pathak and Hiratsuka 2011; Rezaei et al. 2013). This method can be used to cope with vaguely defined classes or categories by making it possible to define the ''membership degree'' of an element in a set by means of a membership function. Pacheco and Sanches Fernandes (2013) used a multivariate statistical method (called Correspondence Analysis) in which the rationale for the adjustment of factor weights is the minimization of redundancy between factors. Despite efforts aiming to improve the DRASTIC index to make it more adaptative to the particularities of the studied regions, no attempt has been undertaken so far to develop an operational methodology by evaluating the potential effect of land use on the overall groundwater quality, thus making it possible to select the relevant factors for assessing the intrinsic aquifer vulnerability and to determine their relative importance. The challenge in this way is accentuated when groundwater samples are collected under a variability of aquifer conditions (i.e., various hydraulic conductivity levels, various soil types, etc.). Barbulescu (2020) underlined the necessity of an informed selection of relevant factors when assessing aquifer vulnerability, the proper validation of factor weighting, and the value ranges allocated to factor categories. Consequently, this study aims to develop a reliable methodology for (1) selecting the relevant factors when assessing the intrinsic aquifer vulnerability and (2) determining the relative importance of the selected factors. Our proposed methodology has been developed by using a large data set of porous granular aquifers, which integrates—in addition to some DRASTIC factors—data related to groundwater quality and land use. If the DRASTIC method is used to assess aquifer vulnerability to contamination for a given region, our approach serves an initial step to determine the relevant factors related to the aquifer in question, while the determined relative importance of these factors is used to validate factor weighting. This study does not validate the original DRASTIC ratings and ranges of the factor categories (Aller et al. 1987) and thus developing a comprehensive adapted vulnerability index for the study region, as well as mapping vulnerability, lies beyond the scope of this study.

Data sources

We have based our study on a regional-scale data set acquired during the Quebec government's hydrogeology characterization program—*Programme d'acquisition de connaissances sur les eaux souterraines* (PACES)—undertaken in the Saguenay-Lac-Saint-Jean (SLSJ) region of Quebec, Canada (13,200 km^2) (Fig. 1). A major output of the PACES-SLSJ Project was the development of a comprehensive groundwater data set generated through (1) the cataloging and digitizing of existing relevant information related to regional groundwater; (2) a regional groundwater sampling campaign; and (3) the application of a quality control process to screen the data for accuracy and quality (CERM-PACES 2013). This hydrogeological data set has been used, among others, to build 3D-subsurface hydro-structural models (Chesnaux et al. 2011; Hudon-Gagnon et al. 2015; Foulon et al. 2018); understand the chemical evolution of regional groundwater systems (Walter et al. 2017, 2018, 2019); quantify regional groundwater recharge and water transit times (Chesnaux 2013; Huet et al. 2016; Chesnaux and Stumpp 2018; Boumaiza et al. 2020b, c; Labrecque et al. 2020); characterize the internal architecture of granular aquifers (Boumaiza et al. 2015, 2017, 2019a); perform more realistic analyses of heterogeneous—non purely Theissian—flow systems (Ferroud et al. 2018, 2019); and to identify field evidence of hydraulic connections between bedrock aquifers and the overlying granular aquifers (Richard et al. 2014, 2016a, b). These granular systems in the SLSJ region were deposited following the last deglacial episode, some 11,800 years ago when the SLSJ lowlands were invaded by the Laflamme Sea. The regional SLSJ graben physiography is marked by large accumulations of Quaternary deposits (sand, gravel, and clay-silt) to a thickness of 180 m in the central SLSJ lowlands (Dionne and Laverdière 1969; Lasalle
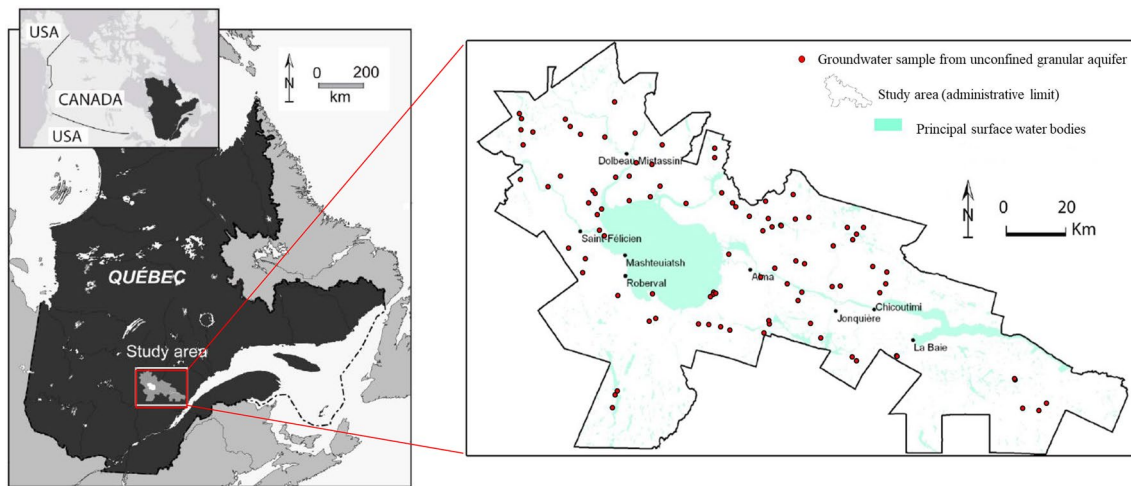
Fig. 1 Location of the study area and the groundwater sampling network sites used to generate the data

and Tremblay 1978). In this study, we used groundwater samples collected as part of the PACES-SLSJ project from the granular unconfined aquifers (Fig. 1).

Description of the developed operational methodology

Our methodology for identifying the relevant factors and their relative importance for assessing aquifer vulnerability is summarized in Fig. 2. We detail the ten methodological steps of Fig. 2 in the following subsections.

Step 1: Selecting an aquifer vulnerability index method

We selected the DRASTIC index for applying our proposed methodology because of the available information related to DRASTIC factors. Nonetheless, our evaluation process is limited to only five DRASTIC factors: the depth of the water table from the ground surface (D); the average annual recharge (R); the dominant aquifer soil type (S); the surface topography expressed as terrain-slope (T); and the average hydraulic conductivity of the aquifer (C). Aquifer type (A) is excluded because our study is restricted to unconfined granular aquifers. Therefore, the impact of the vadose zone (I) was not considered in the present study because the vadose zones of all studied aquifers are dominated by granular material. Information related to the considered factors at the groundwater sampling sites is compiled in Supplementary data (Appendix 1). The methods used for estimating these factors are described in CERM-PACES (2013).

Step 2: Preparing the data set, including groundwater quality and land use

Assessing groundwater quality

We evaluated groundwater quality at the sampling sites using the water quality index (WQI) (Horton 1965). The chemical concentrations of Ca^{2+}, Mg^{2+}, Na^+, HCO_3^-, SO_4^{-2}, Cl^-, F^-, NO_3^-, Fe, Mn, and Zn of 98 groundwater samples were considered (Supplementary data (Appendix 1)). These chemical parameters were selected because their concentrations in groundwater are rarely below the detection limit. We combined these chemical parameters with total dissolved solids (TDS) and pH to evaluate the WQI of each sample for drinking purposes (Horton 1965). To compute WQI, we first calculated the relative weight of each considered chemical parameter using Eq. 1.

$$W_i = \frac{w_i}{\sum_{i=1}^{n} w_i}, \tag{1}$$

where W_i is the relative weight of the chemical parameter, n is the sum of the chemical parameter weights, and w_i is the attributed weight to the chemical parameter (Table 1). We assigned each chemical parameter a value for w_i between 1 (least effect on water quality) to 5 (greatest effect on water quality) on the basis of their perceived effects on primary health and their relative importance on drinking water quality. We assigned the highest weight of 5 to NO_3^- because this parameter has important health effects, whereas the lower weights of 1 and 2 were assigned to Zn, Ca^{2+}, Mg^{2+}, and Na^+ due to their minimal importance in water quality assessments (Ramakrishnaiah et al. 2009; Şener et al. 2017; Sethy et al. 2017).

Fig. 2 Successive steps of the developed operational methodology. The confirmations YES and NO indicate where a preceding step has been either completed (YES) or remains to be completed (NO)
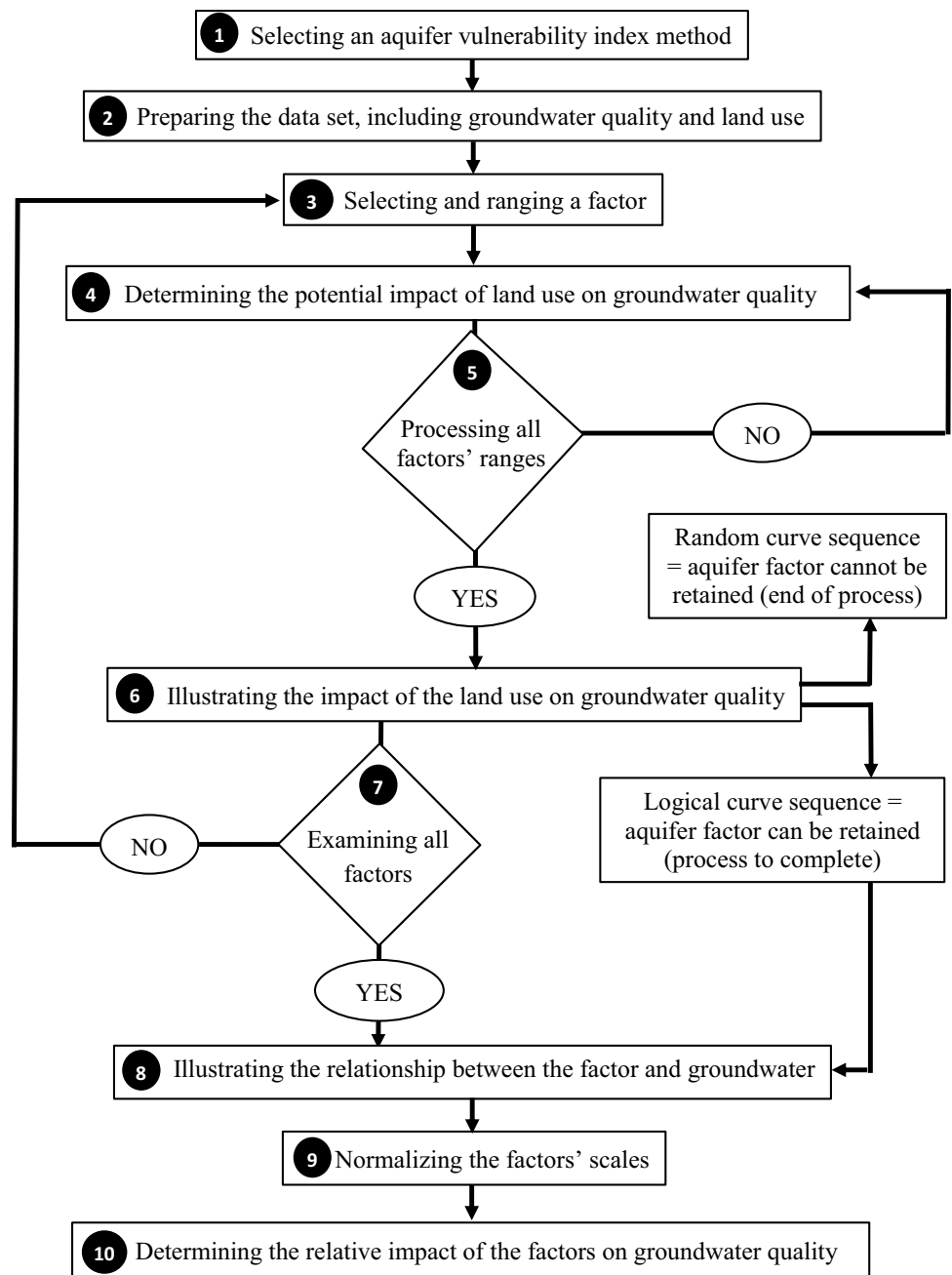
We then calculated the quality rating scale for each chemical parameter using Eq. 2, where q_i is the quality rating scale, C_i is the measured concentration of the chemical parameter (mg/L) in the groundwater sample, and S_i is the drinking water standard concentration (mg/L) for each chemical parameter (Table 1). Finally, we calculated the sub-index (SI_i) for each chemical parameter using Eq. 3, and from this we determined WQI as the sum of the SI_i values (Eq. 4) (Horton 1965). Thus,

$$q_i = \left(\frac{C_i}{S_i} \right).100, \tag{2}$$

$$SI_i = W_i.q_i, \tag{3}$$

$$WQI = \sum SI_i. \tag{4}$$

Table 1 Data used to calculate the relative weights of the chemical parameters

Chemical parameter	Adopted drinking water standard concentration in mg/L (BIS 2012; WHO 2017)	Weight (w_i)	Relative weight (W_i)
pH	7.5	4	0.1
TDS	500	4	0.1
Ca^{2+}	75	2	0.05
Mg^{+2}	30	2	0.05
SO_4^{2-}	200	4	0.1
Cl^-	250	3	0.1
F^-	1	4	0.1
NO_3^-	50	5	0.1
HCO_3^-	200	3	0.1
Na^+	200	2	0.05
Fe	0.3	4	0.1
Mn	0.1	4	0.1
Zn	5	1	0.02
Sum of the chemical parameter weights		42	1

Table 2 Water quality classification

WQI value	Water quality
< 50	Excellent
50–100	Good
100–200	Poor
200–300	Very poor
> 300	Unsuitable

Table 3 Land-use effect level codification

Land use	Assumed potential impact of land use on groundwater quality	Land-use effect level
Forest	Negligible	1
Agricultural	Minor	2
Urban	Moderate	3
Agricultural-urban	High	4
Industrial	Extreme	5

The evolution of groundwater chemistry within geological systems is complex; chemical elements can be present at naturally high concentrations or/and be increased because of anthropogenic stressors (Appelo and Postma 2005). To determine whether the groundwater quality of a site is predominantly affected by geological (i.e., natural) or anthropogenic sources, we applied a Spearman rank correlation coefficient, as this coefficient is not restrained by sample size or the general distribution of variables (Huan et al. 2012). A Spearman rank value of + 1.0 or –1.0 indicates, respectively, a positive or negative correlation between two examined variables, whereas a value of 0.0 indicates no correlation. For all of our sampling sites, the WQI is correlated with the DRASTIC index (CERM-PACES 2013), by assuming that the DRASTIC index represents the geological influence (Heiß et al. 2020). The calculated Spearman rank correlation coefficient was 0.06, suggesting that groundwater contamination within the unconfined aquifers of SLSJ region is not linked (primarily) to regional geology. Thus, we can assume that the WQI of our study region is affected mainly by surface anthropogenic sources, from which the potential contamination is assumed to be transported only vertically, as lateral contaminant transport is neglected in the DRASTIC method. The calculated WQI values for the groundwater samples collected from the unconfined aquifers of SLSJ region are presented in Supplementary data (Appendix 1) and were classified according to Table 2.

Classifying the land-use effect

Comprehensive information on land use across the SLSJ region is available from CERM-PACES (2013). The land-use map, which was produced at the same time as the groundwater sampling campaign, indicated that SLSJ surface areas are occupied by four main sectors: forestry, agricultural, urban, and industrial sectors. Some areas represent mixed agricultural-urban sectors. We proposed a subjective land-use effect to rate the overall effect of land use on groundwater quality (Table 3). Higher values of the land-use effect (on a scale from 1 to 5) reflect a greater land-use influence. The assigned land-use effect levels for the groundwater sampling sites are presented in Supplementary data (Appendix 1). Despite the presence of an industrial sector in the SLSJ region, we did not record a level 5 land-use effect at the locations where the groundwater samples were collected.

Step 3: Selecting and ranging a factor

Step 3 consists of selecting one factor, e.g., hydraulic conductivity, that will be further evaluated in steps 4–9 (Fig. 2). Step 3 also involves, for the selected factor, establishing categories that represent different value ranges, e.g., slope category 1, 0–6%; slope category 2, 6–12% (Table 4). Here, our factor ranges are derived from existing DRASTIC ranges (Aller et al. 1987). A factor range is introduced by dividing each factor into intervals (Table 4) with the aim of determining whether groundwater quality is affected within different factor ranges. For example, aquifers having a lower hydraulic conductivity (Range 1, Table 4) are expected to be less vulnerable than aquifers having a higher hydraulic conductivity (Range 3, Table 4).

Steps 4 and 5: Determining the potential impact of land use on groundwater quality

To identify the variation in groundwater quality in relation to land use, we introduce a mean-weighted WQI (MW_{WQI}) in Step 4. The MW_{WQI} provides a representative indicator of groundwater quality for a set of groundwater samples collected from various locations within the same land-use category. The MW_{WQI} for a given land-use category is calculated using Eq. (5), adapted from Boumaiza et al. (2019a). In this study, P_i is the occurrence probability of WQI class for land-use effect level D_i, where i is the weight (1–5) of the WQI classes (Table 5). P_i is calculated according to Eq. (6), where n_i is the number of groundwater samples within WQI class D_i, and n_t is the total number of groundwater samples, both considered for each land-use effect level. An example of the calculation of MW_{WQI} is presented in Table 5.

$$MW_{WQI} = \sum_{i=1}^{5} P_i \cdot D_i, \tag{5}$$

$$P_i = \frac{n_i}{n_t}. \tag{6}$$

MW_{WQI} is initially calculated for the set of groundwater samples belonging to the same range for a given factor, e.g., groundwater samples collected from sites having a terrain-slope range of 0–6% (Category 1; Table 4), and found within the same land-use category, e.g., a level 1 land-use effect, Table 3. The identical calculation is then undertaken for the set of groundwater samples belonging to the other land-use categories (2–4) of the same factor range, e.g., Category 1. A best-fit curve representing the calculated MW_{WQI} versus the land-use effect levels is then traced. This traced best-fit curve shows the variation in groundwater quality—evaluated using the MW_{WQI}—on the basis of the variation in land-use effect levels within a single factor's range. Finally, Step 5 (Fig. 2) performs the identical Step 4 process, although for all ranges of this factor.
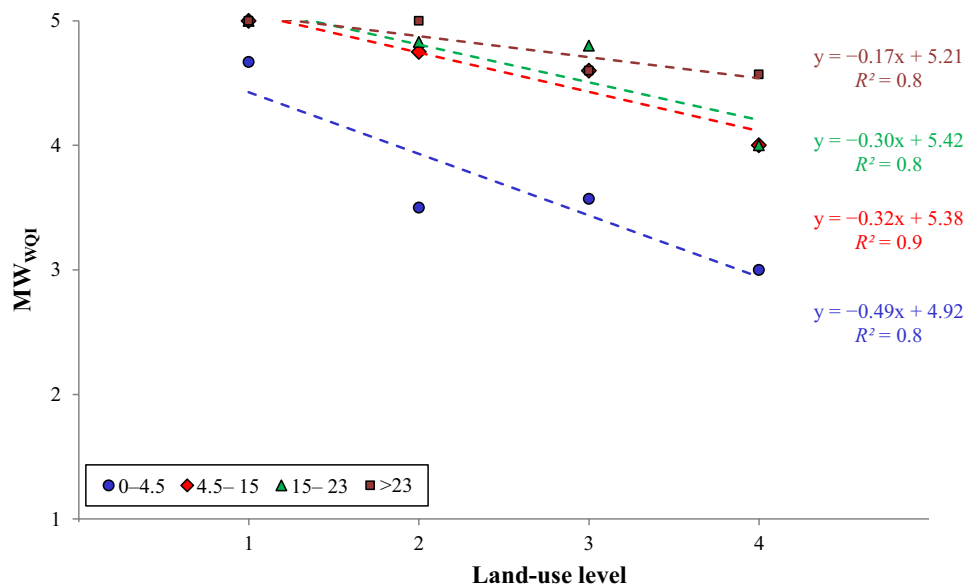
Steps 6 and 7: Illustrating the impact of land use on groundwater quality

Once the calculations are completed in Step 5, the next step consists of drawing all the best-fit curves that represent the calculated MW_{WQI} versus the land-use effect levels. Curves are drawn according to the different ranges of the factor (see an example of the generated best-fit curves in Fig. 3). These best-fit curves represent the groundwater

Table 4 Ranges of the aquifer factors

Factor range	Category
Depth of water table from the ground surface (m)	
0–4.5	1
4.5–15	2
15–23	3
> 23	4
Average annual recharge (mm/year)	
0–100	1
100–180	2
180–250	3
> 250	4
Dominant aquifer soil type[a]	
Gravel	1
Sand	2
Clay-loam	3
Topography – terrain-slope (%)	
0–6	1
6–12	2
12–18	3
> 18	4
Mean aquifer hydraulic conductivity (cm/s)	
$0–5.2 \times 10^{-3}$	1
5.2×10^{-3} to 9.5×10^{-2}	2
$> 9.5 \times 10^{-2}$	3

[a]On the basis of the dominant soils as described in CERM-PACES (2013)

Table 5 Example of calculating MW_{WQI}

WQI class	D_i	n_i
Unsuitable	1	3
Very poor	2	3
Poor	3	1
Good	4	1
Excellent	5	0
	n_t	8
	MW_{WQI}	2

Fig. 3 Groundwater contamination sensitivity curves based on water table depth. Each best-fit line and its equation correspond to the range symbol of the same color in the legend

Legend: 0–4.5, 4.5–15, 15–23, >23

$y = -0.17x + 5.21$
$R^2 = 0.8$

$y = -0.30x + 5.42$
$R^2 = 0.8$

$y = -0.32x + 5.38$
$R^2 = 0.9$

$y = -0.49x + 4.92$
$R^2 = 0.8$

contamination sensitivity curves based on the factor (GCSC/AF sensitivity curves). Step 7 (Fig. 2) involves the identical process—described in steps 3 to 6—for each of the analyzed factors (water table depth, average annual recharge, soil type, terrain-slope, and aquifer hydraulic conductivity). For a given factor, GCSC/AF sensitivity curves should plot in a sequential order related to the factor ranges, and show a logical sequence, as observed in Fig. 3. Here, we refer to a logical sequence as GCSC/AF sensitivity curves plotting in an increasing or decreasing order relative to the factor's ranges. If the GCSC/AF sensitivity curves of a given factor do not show a logical sequence, we reject this factor and do not analyze it in the subsequent steps 8–10 (Fig. 2).

Steps 8 and 9: Illustrating the relationship between factor and groundwater quality

In Step 8, we illustrate the relationship between the factor and groundwater quality; such a process permits the comparison of all analyzed factors in Step 10 (Fig. 2). For this step, the produced GCSC/AF sensitivity curves are converted to groundwater contamination sensitivity curves according to land use (GCSC/LU sensitivity curves). Here, the MW_{WQI} is evaluated from the fitted GCSC/AF sensitivity curves, rather than using the original values, for each land-use effect level (1–4) according to each factor's range. Afterward, we plot the assessed MW_{WQI} values—for each land-use effect level—against the factor's ranges to produce the GCSC/LU sensitivity curves. The ranges of the factor in the GCSC/LU sensitivity curves are represented by a single average value (see an example of the generated GCSC/LU sensitivity curves in Fig. 8a). The process is repeated for the other factors, except for the dominant aquifer soil type (Table 4).

This latter factor is represented by single values of 1, 2, and 3, which correspond to gravel, sand, and loam-clay, respectively. As the factors are expressed in the GCSC/LU sensitivity curves at different scales, i.e., water table depth (m), recharge (mm/years), soil type (grade number), terrain-slope (%), and hydraulic conductivity (cm/s), Step 9 (Fig. 2) involves mathematically normalizing these differing scales. The normalization process is undertaken by subtracting the mean value from the obtained value and then dividing the result by the standard deviation. With a normalized scale, the GCSC/LU sensitivity curves of the various factors can be compared with each other in Step 10.

Step 10: Determining the impact of the factors on groundwater quality

If we assume that groundwater quality has a relationship with the factor, e.g., a water table depth increase causes the MW_{WQI} to increase, the curves linking a factor to groundwater quality (GCSC/LU sensitivity curves) should be illustrated in the form of a slope. Steeper slopes for the GCSC/LU sensitivity curves, including a large MW_{WQI} interval, indicate that the associated factor is more sensitive to the land-use effect level than lower-slope GCSC/LU sensitivity curves. Hence, the factor showing the steepest GCSC/LU sensitivity curve has the greatest effect on groundwater quality. Such slopes vary for each factor, however, as a function of land-use category. Our approach differentiates the effect of each factor—and also considers slope variations in relation to the land-use category—by determining the slope for each GCSC/LU sensitivity curve. Subsequently, plotting the calculated slope versus the considered land-use effect levels,

i.e., 1, 2, 3, and 4, identifies the relative impact of the factors (the generated view is shown in Fig. 10).
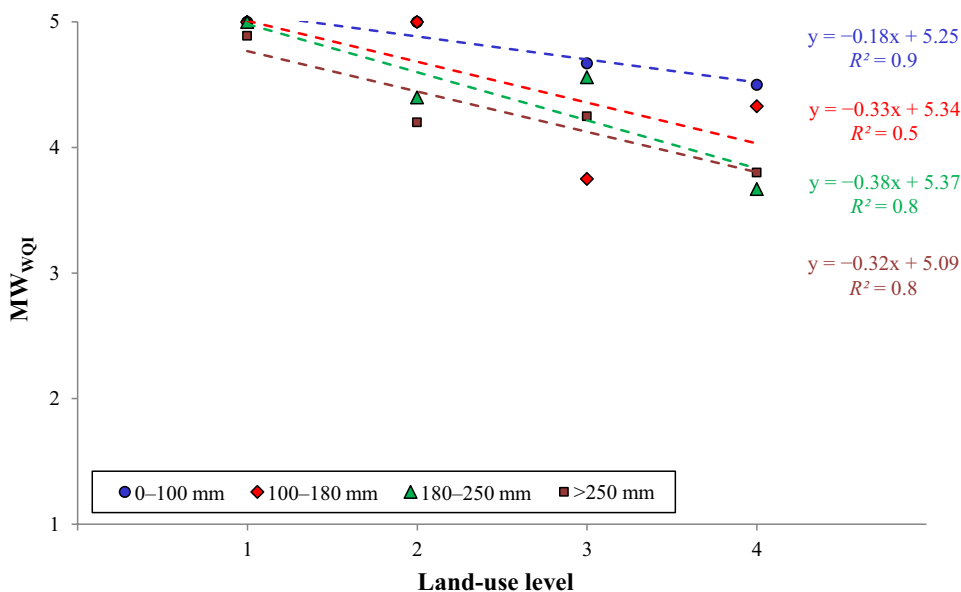
Results

We applied our approach to the regional-scale groundwater data set of the SLSJ region. Our methodology produced: (1) GCSC/AF sensitivity curves in Step 6 (Figs. 3, 4, 5, 6, 7); (2) GCSC/LU sensitivity curves in Step 8 (Fig. 8); normalized GCSC/LU sensitivity curves in Step 9 (Fig. 9); and (3) curves used to determine the relative effect of the factors in Step 10 (Fig. 10).

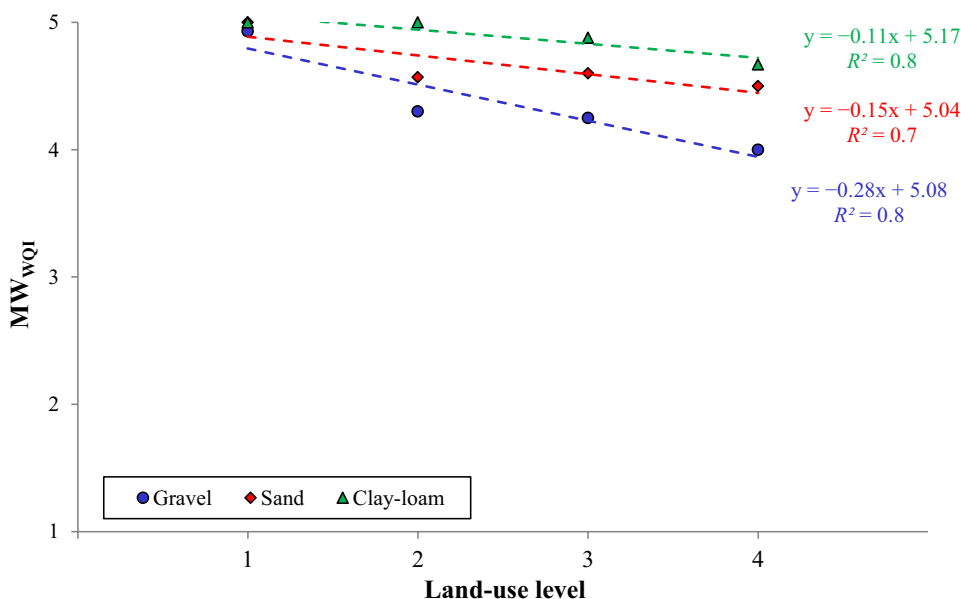## Groundwater contamination sensitivity curves per factor

Water table depth

Aquifers characterized by a water table depth of category 1 (0–4.5 m) are considered more vulnerable to groundwater contamination than aquifers having a greater water table depth, e.g., category 4 (> 23 m). Groundwater contamination sensitivity curves based on water table depth (Table 4) show an inverse relationship between MW_{WQI} and the land-use effect level, i.e., when land-use effect level increases, the MW_{WQI} decreases (Fig. 3). This pattern is expected
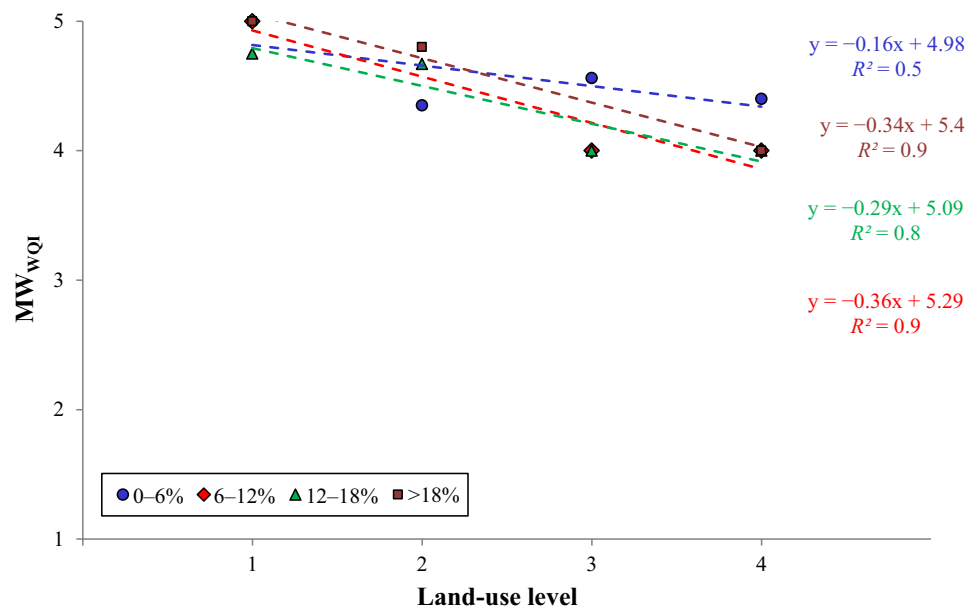

Fig. 4 Groundwater contamination sensitivity curves based on the average annual recharge. Each best-fit line and its equation correspond to the range symbol of the same color in the legend

$y = -0.18x + 5.25$
$R^2 = 0.9$

$y = -0.33x + 5.34$
$R^2 = 0.5$

$y = -0.38x + 5.37$
$R^2 = 0.8$

$y = -0.32x + 5.09$
$R^2 = 0.8$

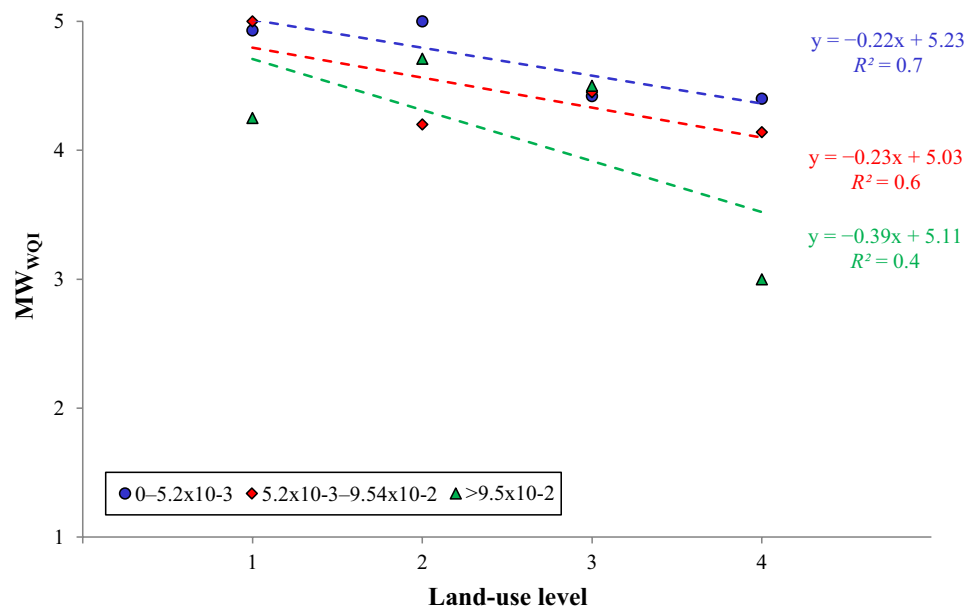Legend: ● 0–100 mm ◆ 100–180 mm ▲ 180–250 mm ■ >250 mm

Fig. 5 Groundwater contamination sensitivity curves based on the dominant vadose zone soil type. Each best-fit line and its equation correspond to the range symbol of the same color in the legend

$y = -0.11x + 5.17$
$R^2 = 0.8$

$y = -0.15x + 5.04$
$R^2 = 0.7$

$y = -0.28x + 5.08$
$R^2 = 0.8$

Legend: ● Gravel ◆ Sand ▲ Clay-loam

Fig. 6 Groundwater contamination sensitivity curves based on terrain-slope (topography). Each best-fit line and its equation correspond to the range symbol of the same color in the legend

$y = -0.16x + 4.98$
$R^2 = 0.5$

$y = -0.34x + 5.4$
$R^2 = 0.9$

$y = -0.29x + 5.09$
$R^2 = 0.8$

$y = -0.36x + 5.29$
$R^2 = 0.9$

Legend: ● 0–6% ◆ 6–12% ▲ 12–18% ■ >18%

Fig. 7 Groundwater contamination sensitivity curves based on the mean hydraulic conductivity of the aquifer. Each best-fit line and its equation correspond to the range symbol of the same color in the legend

$y = -0.22x + 5.23$
$R^2 = 0.7$

$y = -0.23x + 5.03$
$R^2 = 0.6$

$y = -0.39x + 5.11$
$R^2 = 0.4$

Legend: ● 0–5.2x10-3 ◆ 5.2x10-3–9.54x10-2 ▲ >9.5x10-2

because a heightened land-use effect corresponds to an increased potential for groundwater contamination (Table 3), whereas the MW_{WQI} decrease corresponds to a degradation of groundwater quality (see D_i in Table 5). Furthermore, these groundwater contamination sensitivity curves (Fig. 3) follow a logical sequence, i.e., groundwater samples of category 4 (water table depth > 23 m; Table 4) are least sensitive to contamination, and sensitivity is subsequently greater as water table depth decreases. For the land-use effect level 4, for example, a category 1 water table depth (0–4.5 m) has a MW_{WQI} of approximately 3 (poor; Table 5), whereas a category 3 water table depth (15–23 m) has a MW_{WQI} of approximately 4 (good; Table 5). Given that the groundwater

contamination sensitivity curves based on water table depth show a logical sequence and demonstrate an inverse relationship between MW_{WQI} and land-use effect level, we retained water table depth as a relevant factor for assessing aquifer vulnerability to contamination, and this factor is processed in steps 8–10 of our proposed methodology (Fig. 2).

Average annual recharge

Groundwater contamination sensitivity curves based on average annual recharge (Table 4) are aligned in a logical sequence (Fig. 4). Groundwater samples collected from locations having a lower average annual recharge
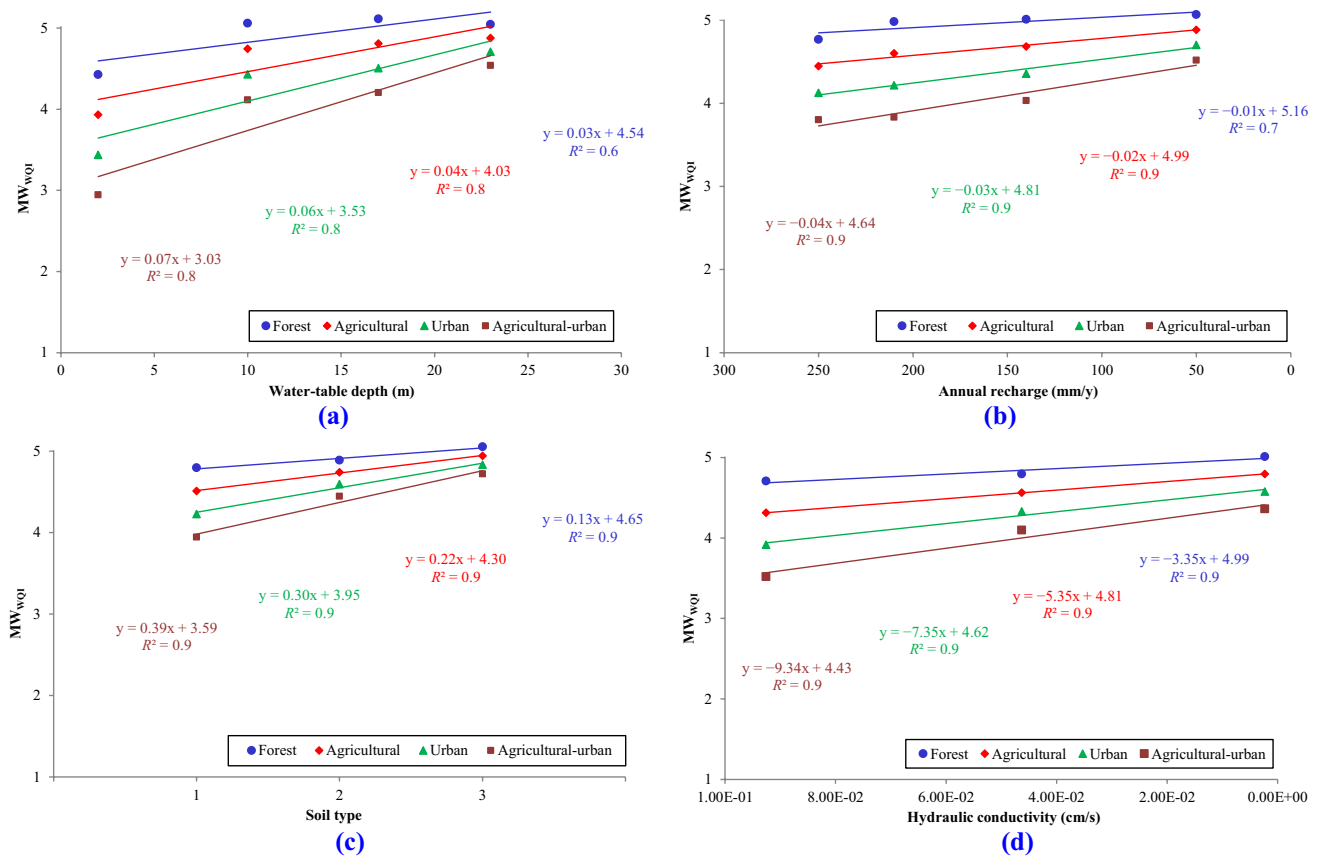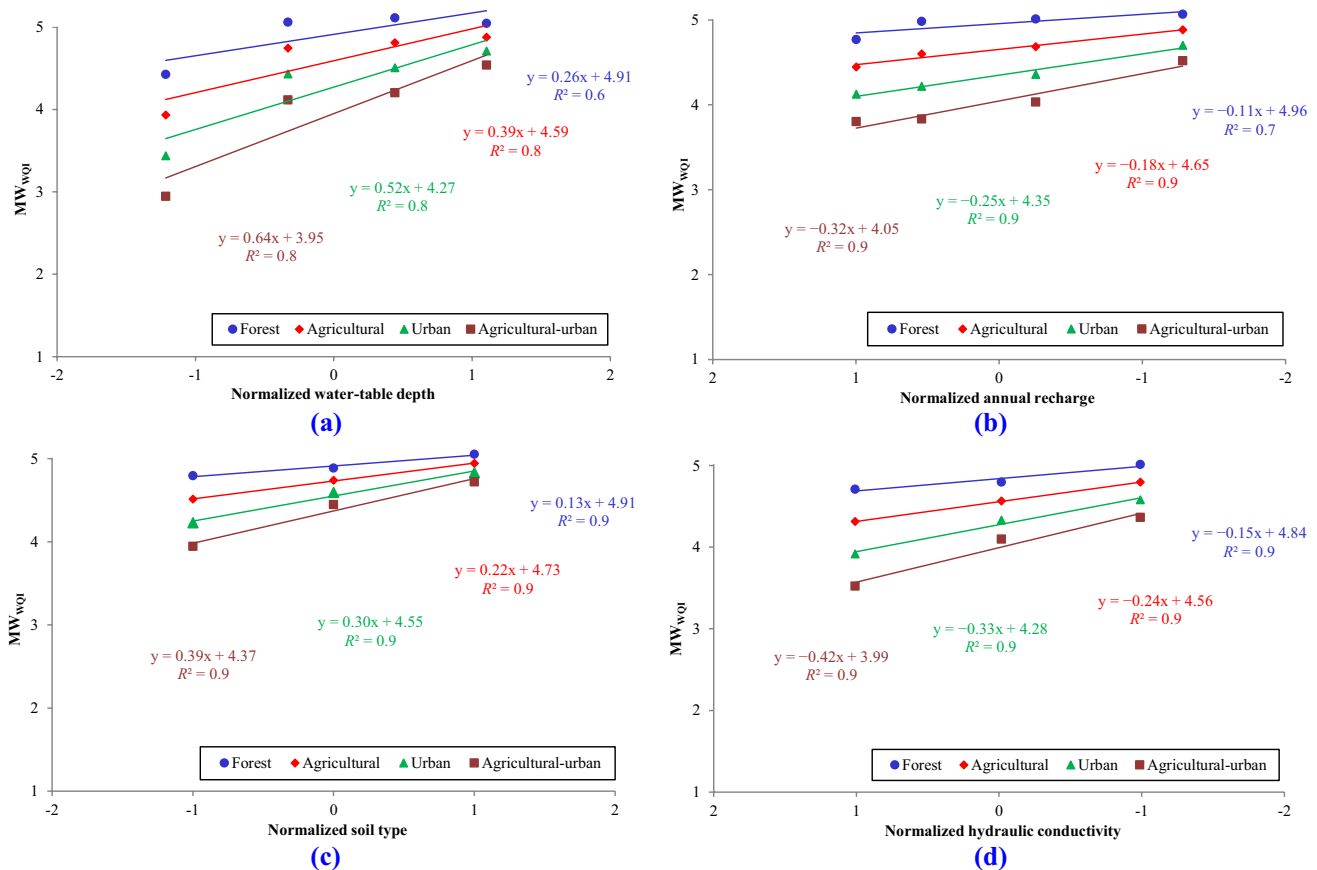
Fig. 8 Groundwater contamination sensitivity curves according to the land-use effect level for **a** water table depth, **b** average annual recharge, **c** dominant vadose zone soil type, and **d** mean hydraulic conductivity of the aquifer. Note that for the sensitivity curves of the average annual recharge and the average aquifer's hydraulic conductivity, the x-axis values are presented from higher to lower values

(0–100 mm/year) are least sensitive to contamination, and sensitivity to contamination increases as average annual recharge increases. For a land-use effect level 3, for example, groundwater sampling locations characterized by an average annual recharge of category 1 (0–100 mm/year) have a MW_{WQI} of approximately 5 (excellent; Table 5), whereas those having an average annual recharge of category 4 (> 250 mm/year) have a MW_{WQI} of approximately 4 (good; Table 5). In a manner similar to the effect of varying water table depth, Fig. 4 shows that when the land-use effect level increases, the MW_{WQI} decreases. That is, there is an inverse relationship between the MW_{WQI} and land-use effect level. As groundwater contamination sensitivity curves show a logical sequence and express a clear inverse relationship between the MW_{WQI} and land-use effect level, we considered the average annual recharge to be a relevant factor in the assessment of vulnerability to contamination. We, therefore, processed this factor in steps 8–10 (Fig. 2).

Dominant vadose zone soil type

In Fig. 5, groundwater contamination sensitivity curves based on the dominant vadose zone soil type (Table 4) illustrate that groundwater samples collected from locations having a vadose zone dominated by clay-loam are least sensitive to contamination, and sensitivity increases (as MW_{WQI} decreases) as the vadose zone becomes increasingly dominated by highly permeable material. We observe a logical sequence of the traced sensitivity curves to contamination: clay-loam is least sensitive, followed by sand. Gravel is most sensitive to contamination (Fig. 5). Groundwater contamination sensitivity curves based on the dominant vadose zone soil type show an inverse relationship between the MW_{WQI} and land-use effect level (Fig. 5), meaning that the increase of the land-use effect level involves a decrease of MW_{WQI}. We, therefore, retained the dominant vadose zone soil type as a relevant factor and processed this factor in steps 8–10 (Fig. 2).

Fig. 9 Normalized groundwater contamination sensitivity curves according to the land-use effect level for **a** water table depth, **b** average annual recharge, **c** dominant vadose zone soil type, and **d** average hydraulic conductivity of the aquifer. Note that the x-axis values are presented from higher to lower values for the average annual recharge and the average hydraulic conductivity of the aquifer

Terrain-slope

According to the followed methodology, groundwater contamination sensitivity curves based on the slope of the land surface (Table 4) show that when the land-use effect level increases, MW_{WQI} decreases by illustrating an inverse relationship (Fig. 6). However, we also observe in Fig. 6 that category 3 (12–18%) is the most sensitive curve to contamination by considering the lower MW_{WQI}. This result is not expected as the highest slope should have a lower recharge and more overland flow and, consequently, a lower contaminant transport leading to a lower sensitivity to contamination. As well, the least sensitive curve to contamination is not clear in Fig. 6, as curves related to categories 1 (0–6%) and 4 (> 18%) intersect. We also

observe random patterns between categories 1 (0–6%) and 2 (6–12%). Hence, these developed curves are not sensitive to the slope. From these observations, we, therefore, eliminate slope as a relevant factor and do not process this factor in steps 8–10 (Fig. 2).

Mean hydraulic conductivity

In Fig. 7, groundwater contamination sensitivity curves based on the average hydraulic conductivity of the aquifer (Table 4) show an inverse relationship between the MW_{WQI} and land-use effect level, i.e., when the land-use effect level increases, the MW_{WQI} decreases. Furthermore, the produced sensitive curves to contamination follow a logical sequence, i.e., groundwater samples

Table 6 Determined slope of the normalized GCSC/LU sensitivity curves

Factor	Land-use effect level	GCSC/ LU slope[a]
Water table depth	1	0.26
	2	0.39
	3	0.52
	4	0.64
Average annual recharge	1	0.11
	2	0.18
	3	0.25
	4	0.32
Dominant vadose zone soil type	1	0.13
	2	0.22
	3	0.30
	4	0.39
Average aquifer hydraulic conductivity	1	0.15
	2	0.24
	3	0.33
	4	0.42

[a]Determined from the normalized GCSC/LU sensitivity curves (Fig. 9)
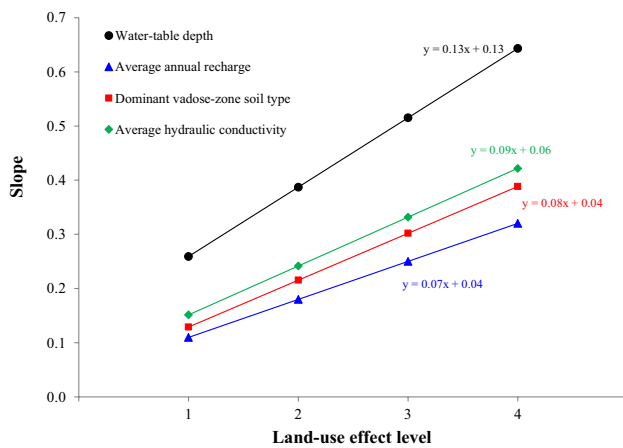
Fig. 10 Slope-variation curves for the determined relevant factors

collected from aquifer locations characterized as category 1 (0–5.2×10^{-3} cm/s; Table 4) are least sensitive to contamination, and sensitivity is greater as the aquifer's hydraulic conductivity increases. For the land-use effect level 2; for example, a category 1 hydraulic conductivity

would produce a MW_{WQI} of approximately 5 (excellent; Table 5), whereas a category 3 hydraulic conductivity (5.2×10^{-3}–9.5×10^{-2} cm/s) results in a MW_{WQI} of approximately 4 (good; Table 5). Given the logical sequence of these curves and the clear inverse relationship between the MW_{WQI} and land-use effect level, we retained average hydraulic conductivity as a relevant factor and processed this factor in steps 8–10.

Groundwater contamination sensitivity curves according to land use

From the retained GCSC/AF sensitivity curves (Figs. 3, 4, 5, 7), we determined the MW_{WQI} for each land-use effect level (1–4) according to the range of each factor. We then traced the GCSC/LU sensitivity curves by plotting the determined MW_{WQI} values—for each land-use effect level—versus the range of each factor. Note that the factor in the GCSC/LU sensitivity curves is represented by a single mean value, except for the dominant aquifer soil type (Table 4), represented by single values of 1, 2, and 3, which correspond to gravel, sand, and loam-clay, respectively. We then normalized the scale of each factor. The results of this processing (Steps 8 and 9) are shown in Figs. 8 and 9.

Determining the relative impact of the factors

The determined slopes for each land-use category in Fig. 9 are presented in Table 6. For each factor, we then plotted the calculated slope versus the considered land-use effect levels, i.e., 1, 2, 3, and 4, to determine the relative impact of the factors (Fig. 10). For the land-use effect level 1, the slopes of the GCSC/LU sensitivity curves (Table 6) of the retained factors were ranked as water table depth (0.26), average hydraulic conductivity (0.15), dominant vadose zone soil type (0.13), and the average annual recharge (0.11). We observed the same pattern of relative ranking for the other land-use effect levels 2, 3, and 4 (Table 6; Fig. 10). Water table depth produced the highest slope values (Fig. 10). Consequently, this factor was considered to have a greater role in controlling groundwater vulnerability to contamination than the other retained factors. Each factor also showed a distinct slope-variation curve, i.e., the line connecting the determined slopes for each land-use effect level (Fig. 10). We note that each produced curve has a specific slope across the land-use effect levels (1–4), which can be ranked (from highest to lowest) as water table depth (0.13), average

hydraulic conductivity (0.09), dominant vadose zone soil type (0.08), and average annual recharge (0.07). This ranking agrees with the relative importance ranking of the factor. In terms of relative importance, the analyzed factors were ranked in importance (from highest to lowest) as (1) water table depth, (2) average hydraulic conductivity, (3) dominant vadose zone soil type, and (4) average annual recharge.

Validation

We can validate our methodology by applying the developed GCSC/LU sensitivity curves (Fig. 9) to external data and verify whether our obtained GCSC/LU for a given factor (Fig. 9) can reliably predict MW_{WQI}. For this purpose, we selected the GCSC/LU sensitivity curves related to water table depth (Fig. 8a) and used data from 22 groundwater samples collected from the granular unconfined aquifers of the Charlevoix-Haute-Côte-Nord (CHCN) region of Quebec (CERM-PACES 2015). This region experiences similar climatic conditions as those of the nearby SLSJ region, and

the available data set provided complete information for each site, including water chemistry, land-use effect level, and water table depth (see Supplementary data (Appendix 1). Groundwater samples used for this validation are identified by the prefix CHCN. We then calculated the WQI of the 22 selected groundwater samples from the chemistry data and expressed the results according to the ranking proposed in Table 5 (this weighted-WQI, hereinafter called the measured-W_{WQI}). We combined water table depths and land-use effect levels of the 22 groundwater samples in Fig. 8a to determine a synthetic value for WQI (this synthetic weighted-WQI is called hereinafter the predicted-W_{WQI}). We note that the predicted-W_{WQI} agrees with the measured-W_{WQI} for 15 (68%) groundwater samples (Table 7). Nonetheless, seven (32%) groundwater samples have a predicted-W_{WQI} that differs from the measured-W_{WQI}. We used the root mean square error (RMSE) to evaluate the effectiveness of the obtained results, as RMSE is often used in geosciences to assess the test quality both in terms of accuracy and precision (e.g., Chesnaux et al. 2017; Boumaiza et al.

Table 7 The calculated RMSE as part of the validation process

ID	Computed WQI	Corresponding WQI class	Measured-W_{WQI}	Predicted-W_{WQI}[a]	Max. Predicted-W_{WQI}
CHCN016	16	Excellent	5	5	1
CHCN025	19	Excellent	5	5	1
CHCN026	28	Excellent	5	4	1
CHCN027	18	Excellent	5	5	1
CHCN028	19	Excellent	5	4	1
CHCN031	16	Excellent	5	5	1
CHCN032	31	Excellent	5	4	1
CHCN034	18	Excellent	5	5	1
CHCN035	15	Excellent	5	5	1
CHCN038	26	Excellent	5	5	1
CHCN039	61	Good	3	3	1
CHCN041	13	Excellent	5	5	1
CHCN051	15	Excellent	5	5	1
CHCN057	43	Excellent	3	3	1
CHCN059	17	Excellent	5	5	1
CHCN063	15	Excellent	5	5	1
CHCN076	50	Excellent	3	4	1
CHCN080	19	Excellent	5	4	1
CHCN084	618	Unsuitable	1	2	5
CHCN086	24	Excellent	5	5	1
CHCN089	25	Excellent	5	4	1
CHCN098	16	Excellent	5	5	1
Real-RMSE				0.7	
Max-RMSE					3.8

[a]Rounded values are determined from the GCSC/LU sensitivity curves in Fig. 8a

2019c). Here, RMSE corresponds to the mean difference between the predicted-W_{WQI}, determined through our developed GCSC/LU sensitivity curves, and the measured-W_{WQI}, computed from the water chemistry data (Eq. 7).

$$\text{RMSE} = \left(\frac{1}{n} \sum_{i=1}^{n} \left(\text{Predicted } W_{WQI} - \text{Measured } W_{WQI}\right)^2\right)^{1/2}. \tag{7}$$

The calculated RMSE (named real-RMSE) indicates the produced error. To determine the maximum possible error that could occur (named max-RMSE), we replaced the predicted-W_{WQI} by the maximum predicted-W_{WQI}, representing a value (1–5). For example, if the measured-W_{WQI} is found to be 2, the maximum predicted-W_{WQI} value that produces max-RMSE is 5. Table 7 presents the real-RMSE and max-RMSE values and shows values of 0.7 and 3.8, respectively. The real-RMSE is lower than the max-RMSE and represents 18.5% of the max-RMSE. With this lower real-RMSE, the actual produced error is considered acceptable relative to the maximum produced error.

Discussion

Our identification of relevant and irrelevant factors agrees with Rupert (1999) who found water table depth, recharge, and soil type to be relevant factors for assessing aquifer vulnerability to contamination. Tesoriero and Voss (1997) also underlined surficial geology as a relevant factor, a factor that can be viewed as a synonym of the dominant vadose zone lithology in our study area. Babiker et al. (2005) used the DRASTIC index to assess aquifer vulnerability; their map sensitivity analysis indicated that the vulnerability index is highly sensitive to recharge, soil type, and topography. This outcome partially agrees with our study, as we also determined recharge and soil type to be relevant factors; however, we did not find topography to be relevant. As in this study, Guo et al. (2007) also found topography to be irrelevant. We also note that for hydraulic conductivity and soil type, these factors are considered irrelevant in some studies (e.g., Panagopoulos et al. 2006), whereas we found them to be relevant for assessing aquifer vulnerability in the SLSJ region. The inclusion or exclusion of factors into the vulnerability assessment process is often related to site-specific conditions and often made on the basis of expert opinion (Worrall et al.

2002). Contradictory evidence in regard to those factors controlling the aquifer vulnerability assessment process has been already noted, particularly when validation is performed for DRASTIC results (Close 1993; Maas et al. 1995). Nonetheless, our ordering of the relative importance of factors (1: water table depth; 2: average hydraulic conductivity; 3: soil type; 4: recharge) largely agrees with the weights in DRASTIC. DRASTIC weights water table depth at 5, hydraulic conductivity at 3, and soil type at 2. Pacheco et al. (2015) found that the importance of water table depth could be reduced (from 5 to 3), whereas the weights of the other factors remain unaltered. In our study, recharge ranks last, whereas in DRASTIC, this factor is the second-most important factor, having a weight of 4 within a weight range of 1 to 5 (Aller et al. 1987). An adapted DRASTIC index for pesticide contamination also allocated a relatively high weight (4) to recharge, but this weight value of 4 lies in the middle of the pesticide-DRASTIC weights ranging from 3 to 5 (Al-Zabet 2002). A common principle is that greater recharge heightens the possibility of contaminant transport within the aquifer. This view is a simplified assumption that ignores potential contaminant and sediment-specific sorption and reaction rates (e.g., Kiecak et al. 2019, 2020). The data used in our study were collected from the SLSJ region; this northern humid region usually experiences a heavy snow accumulation with limited water infiltration during winter/early spring (from November to April). This climatic regime leads to a lower effect of recharge in the eventual transport of intrinsic contamination, as the water available for infiltration into the subsurface is limited for almost half of the year.

We also found terrain-slope (topography) to be an irrelevant factor for assessing the aquifer vulnerability to contamination in the SLSJ region. This factor has commonly been excluded from the DRASTIC index, as the topography of the investigated areas is generally flat (e.g., Khan et al. 2014; Wu et al. 2014; Wang et al. 2017); nonetheless, this exclusion does not hold for regions characterized by a variable topography. The limited effect of the topography in the SLSJ region can be related to the regional climate conditions. The aquifer recharge in the SLSJ region is generally dominated by snowmelt when 5–6 months of accumulated snowpack melts in the spring season to become available for infiltration. Assuming that the snow-melting process first affects the upper snowpack layers (exposed to the sun), the snowpack lower layers can limit water infiltration on both sloped and

flat areas. This mechanism causes the entire region to be, at least temporarily, under similar water infiltrating conditions. Therefore, this scenario limits the importance of surface slope as a controlling factor on aquifer recharge and minimizes the role of topography on aquifer vulnerability. Our operational methodology is intended as an initial step for selecting the relevant factors when assessing aquifer vulnerability and for determining the relative importance of these selected factors. Nonetheless, because the original DRASTIC factor category ranges adopted in our study (Table 4) have not been validated, we cannot propose a DRASTIC-derived index that is adapted to the SLSJ region, nor can we map regional vulnerability. We observed that the sensitivity curves of Figs. 3, 4, 5 and 7 plots in sequential order relative to the factor ranges, although for some cases, the sensitivity curves are quite similar, i.e., nearly overlapping. In Fig. 3, for example, we observe an obvious difference for the water table depth range of 0–4.5 m, whereas the other depth ranges show quite similar curves. Such an observation potentially justifies a re-evaluation of all factor ranges (Table 4) depending on the study site, to validate (1) the number of ranges required for each factor and (2) the limit values attributed to each factor range. We recommend complementary statistically-based studies to determine these range properties. Finally, our study relied on data collected from unconfined aquifers from a northern region characterized by humid climate conditions. This developed operational methodology could be, however, easily adapted to other regions that differ in geological specificities, e.g., confined aquifer, karstic aquifer, etc., and climate conditions, and our approach could also incorporate other available data and factors related to aquifer vulnerability indices. It is, therefore, possible to evaluate whether aquifer vulnerability assessments are affected by other factors not tested here.

Conclusions

In this study, we have presented an operational approach for: (1) selecting the relevant factors when assessing aquifer vulnerability to contamination; and (2) determining the relative importance of the selected factors. We developed our methodology using a large data set from granular aquifers of Saguenay-Lac-Saint-Jean region of Quebec, Canada. The available data included water table depth, average aquifer hydraulic conductivity, topography (terrain-slope), dominant vadose zone soil type, and average annual recharge. We combined these data with information related to groundwater quality and land use. We found topography to be an irrelevant factor for assessing the aquifer vulnerability in our study region. The relevant factors ranked in their relative importance (from highest to lowest) were: (1) water table depth; (2) average aquifer hydraulic conductivity; (3) dominant vadose zone lithology; and (4) average annual recharge. This ranking is representative only for this study region because it is established as a function of the applied data set and cannot be considered as a standard factor ranking. Our results partially agree with the weights of factors in DRASTIC, in which water table depth weight is 5, aquifer hydraulic conductivity is 3, and soil type is 2. Nonetheless, our result for the recharge factor, which we ranked as last, differs from that of the DRASTIC index where recharge was the second-most important factor. This study provides an original approach for integrating groundwater quality data and land-use effects with a data set of the characterized factors, a process that has not been previously applied in the weighting of DRASTIC factors. We do not intend this study to be a comparison with DRASTIC weighting or other methods or an evaluation of the DRASTIC index. Rather, we have introduced an operational methodology that can serve as an initial step for determining relevant the DRASTIC factors for assessing regional aquifer vulnerability. The second step, determining the relative importance of the relevant factors, serves to validate the weight attributed to each DRASTIC factor.

Availability of data and material Supplementary data (Appendix 1) that supports the finding of this study can be found online at https://doi.org/10.1007/s12665-021-09575-w

Code availability Not applicable.

Declarations

Conflict of interest No potential conflict of interest was reported by the authors.

References

Al-Hanbali A, Kondoh A (2008) Groundwater vulnerability assessment and evaluation of human activity impact (HAI) within the Dead Sea groundwater basin, Jordan. Hydrogeol J 16:499–510

Aller L, Bennett T, Lehr JH, et al (1987) DRASTIC : A standardized method for evaluating ground water pollution potential using hydrogeologic settings. Doc. EPA/600/2–87/035. United States Environmental Protection Agency (USEPA), Washington, DC

Al-Zabet T (2002) Evaluation of aquifer vulnerability to contamination potential using the DRASTIC method. Environ Geol 43:203–208

Appelo CAJ, Postma D (2005) Geochemistry, groundwater and pollution, second edition, 2nd edn. Balkema, Leiden

Arauzo M (2017) Vulnerability of groundwater resources to nitrate pollution: a simple and effective procedure for delimiting Nitrate Vulnerable Zones. Sci Total Environ 575:799–812

Awawdeh MM, Jaradat RA (2010) Evaluation of aquifers vulnerability to contamination in the Yarmouk River basin, Jordan, based on DRASTIC method. Arab J Geosci 3:273–282

Baalousha H (2006) Vulnerability assessment for the Gaza Strip, palestine using DRASTIC. Environ Geol 50:405–414

Babiker IS, Mohamed MAA, Hiyama T, Kato K (2005) A GIS-based DRASTIC model for assessing aquifer vulnerability in Kakamigahara heights, gifu prefecture, central Japan. Sci Total Environ 1:127–140

Barbulescu A (2020) Assessing groundwater vulnerability: DRASTIC and DRASTIC-like methods: a review. Water (Switzerland) 12:1356

BIS (Bureau of Indian Standards) (2012) Indian standard drinking water specification. Second Revision ISO: 10500–1012. Drinking Water Sectional Committee, FAD 25. New Delhi, India

Bouchaou L, Michelot JL, Vengosh A et al (2008) Application of multiple isotopic and geochemical tracers for investigation of recharge, salinization, and residence time of water in the Souss-Massa aquifer, southwest of Morocco. J Hydrol 352:267–287

Boumaiza L, Rouleau A, Cousineau PA (2015) Estimation de la conductivité hydraulique et de la porosité des lithofaciès identifiés dans les dépôts granulaires du paléodelta de la rivière Valin dans la région du Saguenay au Québec. In: Proceedings of the 68th Canadian Geotechnical Conference, Quebec City, Quebec, Canada. p 9

Boumaiza L, Rouleau A, Cousineau PA (2017) Determining hydrofacies in granular deposits of the Valin River paleodelta in the Saguenay region of Quebec. In: Proceedings of the 70th Canadian Geotechnical Conference and the 12th Joint CGS/IAH-CNC Groundwater Conference, Ottawa, Ontario, Canada. p 8

Boumaiza L, Saeidi A, Quirion M (2019) A method to determine the relevant geomechanical parameters for evaluating the hydraulic erodibility of rock. J Rock Mech Geotech Eng 11:1004–1018

Boumaiza L, Saeidi A, Quirion M (2019) Determining relative block structure rating for rock erodibility evaluation in the case of non-orthogonal joint sets. J Rock Mech Geotech Eng 11:72–87

Boumaiza L, Rouleau A, Cousineau PA (2019a) Combining shallow hydrogeological characterization with borehole data for determining hydrofacies in the Valin River paleodelta. In: Proceedings of the 72nd Canadian Geotechnical Conference, St-John's, Newfoundland, Canada. p 8

Boumaiza L, Chesnaux R, Drias T et al (2020a) Identifying groundwater degradation sources in a Mediterranean coastal area experiencing significant multi-origin stresses. Sci Total Environ 746:1–20

Boumaiza L, Chesnaux R, Walter J, Stumpp C (2020c) Constraining a flow model with field measurements to assess water transit time through a vadose zone. Groundwater. https://doi.org/10.1111/gwat.13056

Boumaiza L, Chesnaux R, Walter J, Stumpp C (2020b) Assessing groundwater recharge and transpiration in a humid northern region dominated by snowmelt using vadose-zone depth profiles. Hydrogeol J 28:2315–2329

Brindha K, Elango L (2015) Cross comparison of five popular groundwater pollution vulnerability index approaches. J Hydrol 524:597–613

CERM-PACES (2013) Résultats du programme d'acquisition de connaissances sur les eaux souterraines de la région Saguenay-Lac-Saint-Jean. Université du Québec à Chicoutimi, Centre d'études sur les ressources minérales

CERM-PACES (2015) Résultats du programme d'acquisition de connaissances sur les eaux souterraines du territoire de Charlevoix. Université du Québec à Chicoutimi, Charlevoix-Est et La Haute-Côte-Nord. Centre d'études sur les ressources minérales

Chenini I, Zghibi A, Kouzana L (2015) Hydrogeological investigations and groundwater vulnerability assessment and mapping for groundwater resource protection and management: state of the art and a case study. J Afr Earth Sc 109:11–26

Chesnaux R (2013) Regional recharge assessment in the crystalline bedrock aquifer of the Kenogami Uplands, Canada. Hydrol Sci J 58:421–436

Chesnaux R, Stumpp C (2018) Advantages and challenges of using soil water isotopes to assess groundwater recharge dominated by snowmelt at a field study located in Canada. Hydrol Sci J 63:679–695

Chesnaux R, Lambert M, Walter J et al (2011) Building a geodatabase for mapping hydrogeological features and 3D modeling of groundwater systems: application to the Saguenay-Lac-St.-Jean region. Canada Comput Geosci 37:1870–1882

Chesnaux R, Lambert M, Walter J et al (2017) A simplified geographical information systems (GIS)-based methodology for modeling the topography of bedrock: illustration using the Canadian Shield. Appl Geomatics 9:61–78

Civita M, De Maio M (2004) Assessing and mapping groundwater vulnerability to contamination: the Italian "combined" approach. Geofísica Internacional 43:513–532

Close ME (1993) Assessment of pesticide contamination of groundwater in New Zealand: results of groundwater sampling. NZ J Mar Freshwat Res 27:267–273

Dionne JC, Laverdière C (1969) Sites fossilifères du golfe de Laflamme. Rev Géogr Montréal 23:259–270

Doerfliger N, Jeannin PY, Zwahlen F (1999) Water vulnerability assessment in karst environments: a new method of defining protection areas using a multi-attribute approach and GIS tools (EPIK method). Environ Geol 39:165–176

Erostate M, Huneau F, Garel E et al (2018) Delayed nitrate dispersion within a coastal aquifer provides constraints on land-use

evolution and nitrate contamination in the past. Sci Total Environ 644:928–940

Ferroud A, Chesnaux R, Rafini S (2018) Insights on pumping well interpretation from flow dimension analysis: the learnings of a multi-context field database. J Hydrol 556:449–474

Ferroud A, Chesnaux R, Rafini S (2019) Drawdown log-derived analysis for interpreting constant-rate pumping tests in inclined substratum aquifers. Hydrogeol J 27:2279–2297

Foster S (1987) Fundamental concepts in aquifer vulnerability, pollution risk and protection strategy. In: Duijvenbooden W van, Waegeningh HG van (eds) TNO Committee on Hydrological Research, The Hague. Vulnerability of soil and groundwater to pollutants, Proceedings and Information. 38: 69–86

Foster S, Hirata R, Andreo B (2013) The aquifer pollution vulnerability concept: Aid or impediment in promoting groundwater protection? Hydrogeol J 21:1389–1392

Foulon T, Saeidi A, Chesnaux R et al (2018) Spatial distribution of soil shear-wave velocity and the fundamental period of vibration—a case study of the Saguenay region, Canada. Georisk 12:74–86

Fritch TG, McKnight CL, Yelderman JC, Arnold JG (2000) An aquifer vulnerability assessment of the paluxy aquifer, central Texas, USA, using GIS and a modified DRASTIC approach. Environ Manage 25:337–345

Fusco F, Allocca V, Coda S et al (2020) Quantitative assessment of specific vulnerability to nitrate pollution of shallow alluvial aquifers by process-based and empirical approaches. Water (Switzerland) 12:1–23

Gogu RC, Dassargues A (2000) Current trends and future challenges in groundwater vulnerability assessment using overlay and index methods. Environ Geol 39:549–559

Guo Q, Wang Y, Gao X, Ma T (2007) A new model (DRARCH) for assessing groundwater vulnerability to arsenic contamination at basin scale: a case study in Taiyuan basin, northern China. Environ Geol 52:923–932

Hasiniaina F, Zhou J, Guoyi L (2010) Regional assessment of groundwater vulnerability in Tamtsag basin, Mongolia using DRASTIC model. J Am Sci 6:65–78

Heiß L, Bouchaou L, Tadoumant S, Reichert B (2020) Index-based groundwater vulnerability and water quality assessment in the arid region of Tata city (Morocco). Groundw Sustain Dev 10:1–12

Horton RK (1965) An index number system for rating water quality. J Water Pollut Control Feder 37:300–305

Huan H, Wang J, Teng Y (2012) Assessment and validation of groundwater vulnerability to nitrate based on a modified DRASTIC model: a case study in Jilin City of northeast China. Sci Total Environ 440:14–23

Hudon-Gagnon E, Chesnaux R, Cousineau PA, Rouleau A (2015) A hydrostratigraphic simplification approach to build 3D groundwater flow numerical models: example of a Quaternary deltaic deposit aquifer. Environ Earth Sci 74:4671–4683

Huet M, Chesnaux R, Boucher MA, Poirier C (2016) Comparing various approaches for assessing groundwater recharge at a regional scale in the Canadian Shield. Hydrol Sci J 61:2267–2283

Ibe KM, Nwankwor GI, Onyekuru SO (2001) Assessment of ground water vulnerability and its application to the development of protection strategy for the water supply aquifer in Owerri, Southeastern Nigeria. Environ Monit Assess 67:323–360

Iván V, Mádl-Szőnyi J (2017) State of the art of karst vulnerability assessment: overview, evaluation and outlook. Environ Earth Sci 76:1–25

Javadi S, Kavehkar N, Mousavizadeh MH, Mohammadi K (2011) Modification of DRASTIC model to map groundwater vulnerability to pollution using nitrate measurements in agricultural areas. J Agric Sci Technol 13:239–249

Kazakis N, Voudouris KS (2015) Groundwater vulnerability and pollution risk assessment of porous aquifers to nitrate: Modifying the DRASTIC method using quantitative parameters. J Hydrol 525:13–25

Khan A, Khan HH, Umar R, Khan MH (2014) An integrated approach for aquifer vulnerability mapping using GIS and rough sets: study from an alluvial aquifer in North India. Hydrogeol J 22:1561–1572

Kiecak A, Sassine L, Boy-Roura M et al (2019) Sorption properties and behaviour at laboratory scale of selected pharmaceuticals using batch experiments. J Contam Hydrol 225:1–11

Kiecak A, Breuer F, Stumpp C (2020) Column experiments on sorption coefficients and biodegradation rates of selected pharmaceuticals in three aquifer sediments. Water (Switzerland) 12:14

Kumar P, Bansod BKS, Debnath SK et al (2015) Index-based groundwater vulnerability mapping models using hydrogeological settings: a critical evaluation. Environ Impact Assess Rev 51:38–49

Labrecque G, Chesnaux R, Boucher MA (2020) Water-table fluctuation method for assessing aquifer recharge: application to Canadian aquifers and comparison with other methods. Hydrogeol J 28:521–533

Lasalle P, Tremblay G (1978) Dépôts meubles du Saguenay Lac Saint-Jean. Rapport géologique no 191, ministère des Richesses naturelles du Québec, Canada

Liggett JE, Allen DM (2011) Evaluating the sensitivity of DRASTIC using different data sources, interpretations and mapping approaches. Environ Earth Sci 62:1577–1595

Maas RP, Kucken DJ, Patch SC et al (1995) Pesticides in eastern north carolina rural supply wells: land use factors and persistence. J Environ Qual 24:426–431

Machiwal D, Jha MK, Singh VP, Mohan C (2018) Assessment and mapping of groundwater vulnerability to pollution: current status and challenges. Earth Sci Rev 185:901–927

McLay CDA, Dragten R, Sparling G, Selvarajah N (2001) Predicting groundwater nitrate concentrations in a region of mixed agricultural land use: a comparison of three approaches. Environ Pollut 115:191–204

Moore P, John S (1990) SEEPAGE: A system for early evaluation of the pollution potential of agricultural groundwater environments. Northeast Technical Center United States Department of Agriculture, Soil Conservation Service

Neshat A, Pradhan B, Pirasteh S, Shafri HZM (2014) Estimating groundwater vulnerability to pollution using a modified DRASTIC model in the Kerman agricultural area. Iran Environ Earth Sci 71:3119–3131

Pacheco FAL, Sanches Fernandes LF (2013) The multivariate statistical structure of DRASTIC model. J Hydrol 476:442–459

Pacheco FAL, Pires LMGR, Santos RMB, Sanches Fernandes LF (2015) Factor weighting in DRASTIC modeling. Sci Total Environ 505:474–486

Pacheco FAL, Martins LMO, Quininha M et al (2018) Modification to the DRASTIC framework to assess groundwater contaminant risk in rural mountainous catchments. J Hydrol 566:175–191

Panagopoulos GP, Antonakos AK, Lambrakis NJ (2006) Optimization of the DRASTIC method for groundwater vulnerability assessment via the use of simple statistical methods and GIS. Hydrogeol J 14:894–911

Pathak DR, Hiratsuka A (2011) An integrated GIS based fuzzy pattern recognition model to compute groundwater vulnerability index for decision making. J Hydro-Environ Res 5:63–77

Ramakrishnaiah CR, Sadashivaiah C, Ranganna G (2009) Assessment of water quality index for the groundwater in Tumkur taluk, Karnataka state, India. E-J Chem 6:523–530

Rezaei F, Safavi HR, Ahmadi A (2013) Groundwater vulnerability assessment using fuzzy logic: a case study in the zayandehrood aquifers. Iran Environ Manag 51:67–77

Richard SK, Chesnaux R, Rouleau A et al (2014) Field evidence of hydraulic connections between bedrock aquifers and overlying granular aquifers: examples from the Grenville Province of the Canadian Shield. Hydrogeol J 22:1889–1904

Richard SK, Chesnaux R, Rouleau A (2016) Detecting a defective casing seal at the top of a bedrock aquifer. Groundwater 54:296–303

Richard SK, Chesnaux R, Rouleau A, Coupe RH (2016) Estimating the reliability of aquifer transmissivity values obtained from specific capacity tests: examples from the Saguenay-Lac-Saint-Jean aquifers, Canada. Hydrol Sci J 61:173–185

Rosen L (1994) A study of the DRASTIC methodology with emphasis on swedish conditions. Groundwater 32:278–285

Ruopu L, Merchant JW, Chen XH (2014) A geospatial approach for assessing groundwater vulnerability to nitrate contamination in agricultural settings. Water Air Soil Pollut 225:1–17

Rupert M (1999) Improvements to the DRASTIC ground-water vulnerability mapping method. USGS Fact Sheet FS-066–99, Boise, Idaho 1–6

Sadiki ML, Mezouary L, Khomsi A et al (2018) Groundwater protection using DRASTIC vulnerability maps and arcfem tools for perimeter protection: a case study in the charf El Akab Aquifer (Morocco North). Int J Geosci 9:289–307

Saha D, Alam F (2014) Groundwater vulnerability assessment using DRASTIC and Pesticide DRASTIC models in intense agriculture area of the Gangetic plains, India. Environ Monit Assess 186:8741–8763

Saibi H, Ehara S (2008) Hydrogeology and vulnerability assessment of groundwater resources in the Mostaganem plateau, Northwestern Algeria. J Environ Hydrol 16:1–11

Sener E, Davraz A (2013) Assessment of groundwater vulnerability based on a modified DRASTIC model, GIS and an analytic hierarchy process (AHP) method: the case of Egirdir Lake basin (Isparta, Turkey). Hydrogeol J 21:701–714

Şener Ş, Şener E, Davraz A (2017) Evaluation of water quality using water quality index (WQI) method and GIS in Aksu River (SW-Turkey). Sci Total Environ 584–585:131–144

Sethy SN, Syed TH, Kumar A (2017) Evaluation of groundwater quality in parts of the Southern Gangetic Plain using water quality indices. Environ Earth Sci 76:1–15

Shirazi SM, Imran HM, Akib S (2012) GIS-based DRASTIC method for groundwater vulnerability assessment: a review. J Risk Res 15:991–1011

Shrestha S, Kafle R, Pandey VP (2017) Evaluation of index-overlay methods for groundwater vulnerability and risk assessment in Kathmandu Valley. Nepal Sci Total Environ 575:779–790

Singh A, Srivastav SK, Kumar S, Chakrapani GJ (2015) A modified-DRASTIC model (DRASTICA) for assessment of groundwater vulnerability to pollution in an urbanized environment in Lucknow, India. Environ Earth Sci 74:5475–5490

Tesoriero AJ, Voss FD (1997) Predicting the probability of elevated nitrate concentrations in the Puget Sound Basin: implications for aquifer susceptibility and vulnerability. Ground Water 35:1029–1039

Valle Junior RF, Varandas SGP, Sanches Fernandes LF, Pacheco FAL (2014) Groundwater quality in rural watersheds with environmental land use conflicts. Sci Total Environ 493:812–827

Van Stempvoort D, Ewert L, Wassenaar L (1993) Aquifer vulnerability index: a gis - compatible method for groundwater vulnerability mapping. Can Water Resour J 18:25–37

Wachniew P, Zurek AJ, Stumpp C et al (2016) Toward operational methods for the assessment of intrinsic groundwater vulnerability: a review. Crit Rev Environ Sci Technol 46:827–884

Walter J, Chesnaux R, Cloutier V, Gaboury D (2017) The influence of water/rock−water/clay interactions and mixing in the salinization processes of groundwater. J Hydrol 13:168–188

Walter J, Rouleau A, Chesnaux R et al (2018) Characterization of general and singular features of major aquifer systems in the Saguenay-Lac-Saint-Jean region. Can Water Resour J 43:75–91

Walter J, Chesnaux R, Gaboury D, Cloutier V (2019) Subsampling of regional-scale database for improving multivariate analysis interpretation of groundwater chemical evolution and ion sources. Geosciences (Switzerland) 9:1–32

Wang Y, Merkel BJ, Li Y et al (2007) Vulnerability of groundwater in Quaternary aquifers to organic contaminants: a case study in Wuhan City, China. Environ Geol 53:479–484

Wang S, Zheng W, Currell M et al (2017) Relationship between land-use and sources and fate of nitrate in groundwater in a typical recharge area of the North China Plain. Sci Total Environ 609:607–620

WHO (World Health Organization) (2017) Guidelines for drinking-water quality, 4th edition, incorporating the 1st addendum. ISBN: 978-92-4-154995-0

Worrall F, Besien T, Kolpin DW (2002) Groundwater vulnerability: interactions of chemical and site properties. Sci Total Environ 299:131–143

Wu W, Yin S, Liu H, Chen H (2014) Groundwater vulnerability assessment and feasibility mapping under reclaimed water irrigation by a modified DRASTIC Model. Water Resour Manage 28:1219–1234

Zendehbad M, Cepuder P, Loiskandl W, Stumpp C (2019) Source identification of nitrate contamination in the urban aquifer of Mashhad. Iran J Hydrol 25:1–14

Zhou J, Li G, Liu F et al (2010) DRAV model and its application in assessing groundwater vulnerability in arid area: a case study of pore phreatic water in Tarim Basin, Xinjiang, Northwest China. Environ Earth Sci 60:1055–1063